Advanced lab course for Bachelor's students

Experiment T12

Detection principles

February 2018

Contents

General rules of behavior

Before starting with the experiment on one of the most interesting and fascinating thing in the world, it is useful to define the rules that everyone of us has to follow inside and outside the laboratory. **Do not skip this part and do not forget it!**

- Before entering the lab, place the jackets in the dedicated room
- Do not leave food in the wardrobe room. In case you have no place where to leave the not strictly necessary things, ask the supervisors
- Do not touch the radioactive sources with your hands! There are tweezers to move them...
- Always remember your dosimeter that has always to be with you. Attach it to a pocket or wherever you find it comfortable close to your body and do not leave it on the desk or in the bag
- Follow the indication in these instructions so that the apparatus can be preserved intact
- Don't worry about speaking English with the tutors: not a single point will be deduced if you are not confident with the language
- In case you need the tutors for whatever important reason, do not be shy and contact them

And...

... if you believe, like we do, that particle detectors are really cool, come and ask for a thesis in this field: in our institute there are several opportunities!

1. Introduction

This experiment is designed to give you basic knowledge about the working principles of particle detectors. Figure 1.1 shows a cross-sectional view of the Compact Muon

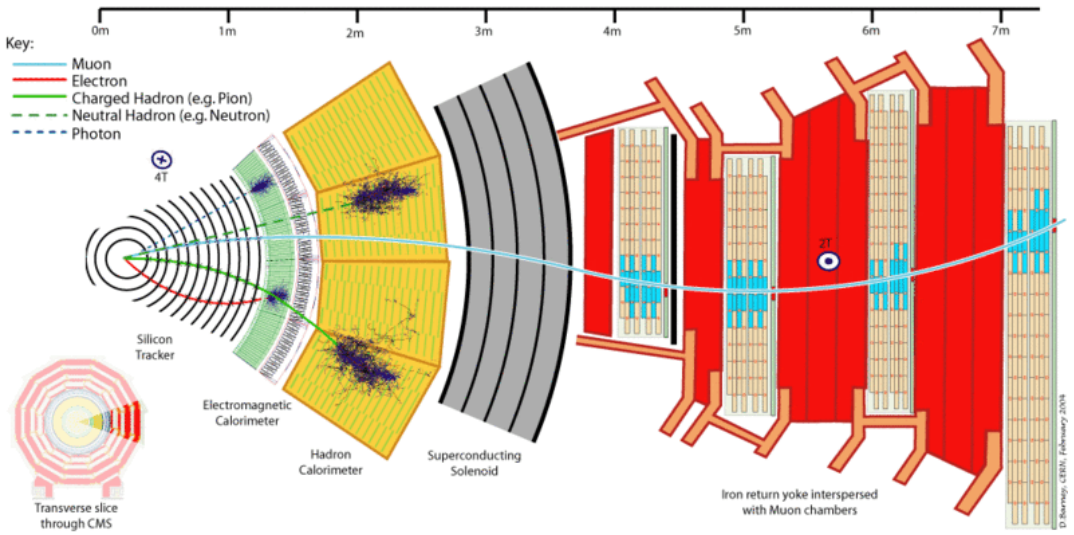

Figure 1.1.: Cross-sectional view of the CMS detector.

Solenoid detector, which is one of the four large experiments at the Large Hadron Collider. There are two basic ways of measuring particle properties.
First, a charged particle momentum may be measured by determining the curvature of its trajectory in a magnetic field. This is e.g. done in the so called tracker, which is a detector with a very good spatial resolution and allows for a precise trajectory measurement. The precision of this process is limited by the influence of multiple scattering due to the material present in the structure of the detectors, which causes a deflection of the particle path.
Second, a calorimeter can be used to measure the energy deposited by a traversing particle, that depends on the particle velocity. In CMS, there is an electromagnetic and a hadronic calorimeter. The electromagnetic calorimeter (ECAL) is used for the detection of photons and electrons/positrons, while the hadronic calorimeter (HCAL) is used to detect hadrons such as protons or kaons.
By determining the energy and the momentum, all the other properties of the particles can be derived, such as the mass and the p_T of the particles.

While in the LHC the particles crossing the detectors are produced making proton beams collide, in this laboratory experiment we will use electrons and positions (e^+, e^-) generated by the β-decay of radioactive sources.

2.1. β-decays

Nuclei with a large imbalance of proton and neutron content decay via the weak interaction. This decay is called β-decay. There are β^-- and β^+- decays, depending on the sign of the β particle generated:

$$n \rightarrow p + e^- + \tilde{\nu} \tag{2.1}$$
$$p \rightarrow n + e^+ + \nu \tag{2.2}$$

The first one occurs in neutron-rich nuclides. A neutron is transformed into a proton, which causes an electron and anti-neutrino to be emitted from the nucleus.
The opposite happen for proton-rich nuclei, which undergo β^+-decays. Here, a proton is transformed into a neutron and a positron and a neutrino are emitted. Energy corresponding to the mass difference between the parent nucleus and its decay products is released. This energy release is typically of the order of 1 MeV.

2.1.1. The β-spectrum

In contrast to the α-spectrum, the β spectrum is not discrete but continuous from zero to the maximal possible energy. The spectrum can be calculated from Fermi "Golden Rule", which describes the transition probability per unit time for a certain initial to final state process:

$$w = \frac{2\pi}{\hbar} \left| \langle \psi_f | \hat{H}_S | \psi_i \rangle \right|^2 \frac{dN}{dE_0} \tag{2.3}$$

$$\psi(\vec{r}) = \frac{1}{\sqrt{V}} e^{\frac{i\vec{p}\cdot\vec{r}}{\hbar}} \tag{2.4}$$

For the β-decay, the transition is from the initial nucleus to the final nucleus plus an anti-neutrino and free electron with a momentum between p_e and $p_e + dp_e$. The transition probability depends on the matrix element and the density $\mathrm{dN/dE_0}$ of possible final

states.
The weak interaction has a very short range and practically only affects the interior of the nucleus. Therefore, the wave function in the matrix element may be approximated using plane waves.

$$exp\left(\frac{i\vec{p}\cdot\vec{r}}{\hbar}\right) \approx 1 + i\frac{\vec{p}\cdot\vec{r}}{\hbar} - \frac{1}{2}\left(\frac{(\vec{p}\cdot\vec{r})}{\hbar}\right)^2 \tag{2.5}$$

Indeed, using $p_e \sim 1$ MeV/c and r $\sim 10^{-15}$ m, we get $\frac{\vec{p_e}\cdot\vec{r}}{\hbar} \approx 10^{-3}$. Assuming that the wave function is approximately constant over the extent of the nucleus, we can write:

$$\left|\langle\psi_f|\,\hat{H}_S\,|\psi_i\rangle\right|^2 = \frac{g^2\,|M_{fi}|^2}{V^2} \tag{2.6}$$

where g is a coupling constant that parametrizes the strength of the weak interaction and $|M_{fi}|$ is the nucleus matrix element containing the wave function. V is a normalizing factor for the wave function.
This equation tells us that electron and neutrino do not carry away any angular momentum. Thus, the transition is allowed (see below).
To calculate the density of allowed final states, we need to take into account that the released energy is shared between electron and neutrino: $E_0 = E_e + E_\nu$. Also, the total momentum of the system must be conserved. The nucleus is much heavier than electron and neutrino, which allows us to neglect the recoil energy carried by it. The total number of states dN is a combination of the electron and neutrino states:

$$dN = \mathrm{dn}_e\mathrm{dn}_\nu \tag{2.7}$$

where location and momentum are related by the uncertainty relation $d^3x d^3p \geq (2\pi\hbar)^3$. Each states occupies a phase volume of h^3, thus the total density of states is:

$$\frac{dN}{dE_0} = \frac{\mathrm{V}}{(2\pi\hbar)^3}4\pi p_e^2 dp_e\,\frac{\mathrm{V}}{(2\pi\hbar)^3}4\pi p_\nu^2\frac{dp_\nu}{dE_0} = \frac{16\pi^2\mathrm{V}^2}{(2\pi\hbar)^6}p_e^2 p_\nu^2\frac{dp_\nu}{dE_0}dp_e \tag{2.8}$$

where we have assumed that the interaction is confined to the volume V. This is possible due to the short range of the weak interaction. Neglecting neutrino masses, we arrive at

$$p_\nu^2 dp_\nu = \frac{(E_0 - E_e)^2}{c^3}dE_0 \tag{2.9}$$

and thus

$$dw(p_e) = \frac{2g^2}{(2\pi)^3\hbar^7 c^3}\,|M_{fi}|^2\,(E_0 - E_e)^2 p_e^2 dp_e = K\,|M_{fi}|^2\,p_e^2(E_0 - E_e)^2 dp_e. \tag{2.10}$$

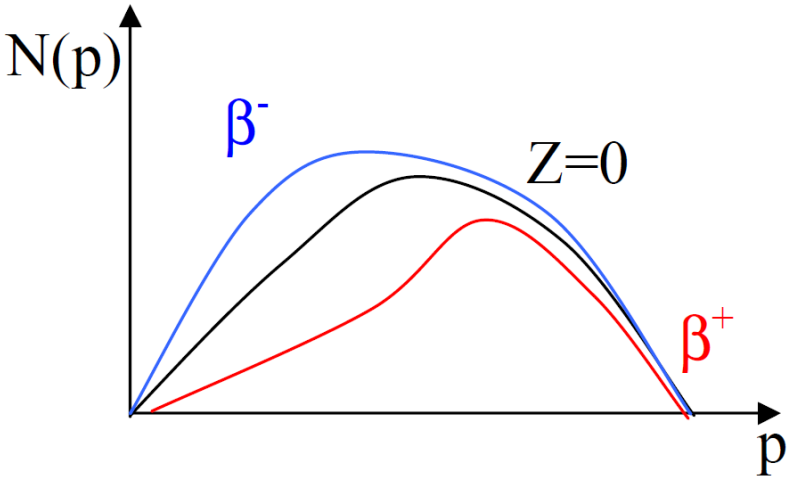

Figure 2.1.: Momentum spectrum with and without Fermi correction.

We can now replace E_e by the kinetic energy of the electron $T_e = E_e - m_e$ as it is measured in the scintillator and dp_e by dT_e, which gives

$$dw(T_e) = K\,|M_{fi}|^2\,(E_{max} - E_e)^2(T_e + m_e)\sqrt{T_e^2 + 2T_e m_e}dT_e \tag{2.11}$$

Note: In literature, it is common to only give the maximal kinetic energy of the electron E_{max} as decay energy.

2.1.2. Fermi correction

Up to this point we have neglected the Coulomb interaction between nucleon and electron/positron. When leaving the nucleon's electromagnetic field, electrons are decelerated and positrons are accelerated. The strength of this effect depends on the nucleon charge number Z and the momentum of the emitted particles. In both cases, the spectrum is distorted as shown in fig. 2.1. This correction is formulated as the ratio of the electron wave functions with and without the effect taken into account.

$$F(Z,\eta) = \frac{2\pi\eta}{1 - e^{-2\pi\eta}}\ ,\ \eta = \pm\frac{Z\alpha E_e}{p_e} \tag{2.12}$$

where + (−) is used for electrons (positrons). F(Z,p_e) is called Fermi function. The differential momentum distribution is then finally

$$\frac{dw}{dp_e} = K\,|M_{fi}|^2\,F(Z,p_e)p_e^2(E_{max} - E_e)^2. \tag{2.13}$$

2.1.3. Allowed and prohibited transitions

In all calculations, we have assumed the matrix element to be constant. However, this is only true for so called "allowed" transitions, where electron and neutrino do not carry angular momentum. Allowed transitions have high transition probabilities. There are two kinds of allowed transitions:

Fermi transition:
The spins of electron and neutrino are aligned in opposite directions. A singlet state ($s_\beta + \bar{s}_\nu = 0$) is formed, the nuclear spin is unchanged ($\Delta J = 0$).

Gamow-Teller transition:
Electron and neutrino form a triplet state ($s_\beta + \bar{s}_\nu = 1$). In this case, the nuclear spin may change by $\Delta J = \pm 1, 0$, where $J = 0 \to J = 0$ is excluded.

The other transitions are called "prohibited". The more prohibited they are, the more the rate is reduced. This means that the electron wave function is not constant over the extent of the nucleus as assumed in eq. 2.5. Therefore, the approximation has to be calculated in higher orders, which changes the matrix element. Whether a decay is prohibited, may be found out by considering the total decay probability per unit time λ. It is calculated by integrating the momentum spectrum over all possible momenta:

$$\lambda = \frac{1}{\tau} = \int_0^{p_{max}} \frac{dw}{dp_e}\, dp_e = K\,|M_{fi}|^2 \int_0^{p_{max}} F(Z, p_e) p_e^2 (E_{max} - E_e)^2\, dp_e \tag{2.14}$$

We define the kinetic energy per electron mass $W_e = \frac{E_e}{m_e c^2}$

$$\lambda = K'\,|M_{fi}|^2 \int_1^{W_{max}} F(Z, W_e) \sqrt{W_e^2 - 1} (W_{max} - W_e)^2\, dW_e \tag{2.15}$$

The integral is also called Fermi integral $f(Z, W_{max})$. It only depends on the nuclear charge Z and W_{max}. We replace the mean lifetime by the half-life:

$$\lambda = \frac{\ln(2)}{t_{1/2}} = K'\ |M_{fi}|^2\ f(Z, W_{max}). \tag{2.16}$$

And we thus arrive at the so called "ft value"

$$f(Z, W_{max}) t_{1/2} = \frac{\ln(2)}{K'\ |M_{fi}|^2}\,, \tag{2.17}$$

which may be used to estimate which class of transition a decay belongs to. It only depends on the matrix element. The value of the Fermi integral $f(Z, W_{max})$ for different

Z and W_{max} can e.g. be found in A.2 in the appendix.
ft values up to 10^6 are considered allowed, larger values are prohibited. The degree of prohibition (single, double, etc.) increases approximately every two orders of magnitude.

What kind of transitions are found in ^{90}Sr and ^{90}Y? ... we are going to use the ^{90}Sr in our experiment!

2.1.4. Kurie diagram

We can now plot $\sqrt{\frac{dw/dp_e}{F(Z,p_e)p_e^2}}$ against the electron's kinetic energy. If $|M_{fi}|^2$ is indeed constant, we expect a linear behavior as shown in 2.2. In this view, the maximal energy is determined by finding the intersection with the x-axis. Additionally, this plot can be used to spot multiple decay components in the spectrum, which lead to kinks in the line.

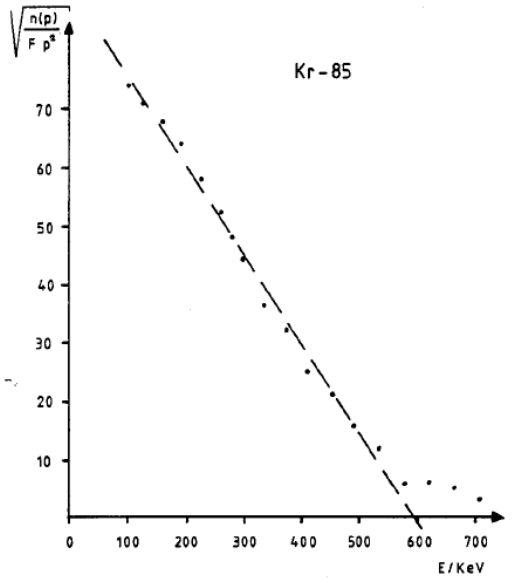

Figure 2.2.: Example Kurie diagram for the energy spectrum of Kr85.

2.2. Bending charged particles in magnetic fields

When an electrically charged particle traverses an electromagnetic fields, it is accelerated as shown in the Lorentz equation 2.18.

$$\vec{F} = q\ (\vec{E} + \vec{v} \times \vec{B}) \tag{2.18}$$

Where q is the particle charge, $\vec{v}$ is its velocity and $\vec{E}$ and $\vec{B}$ are the electric field strength and the magnetic flux density.

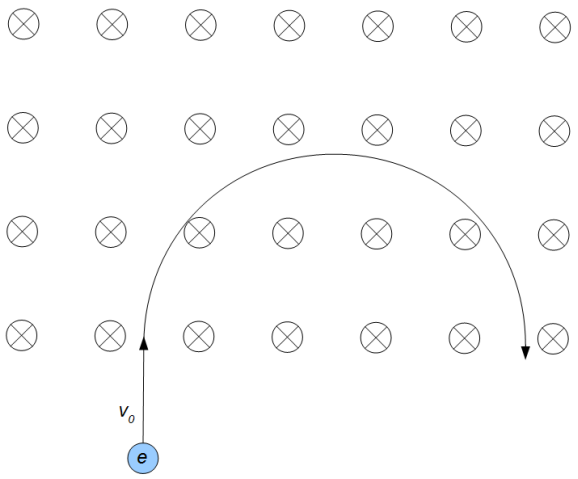

Figure 2.3.: Electron in a constant homogeneous magnetic field

The first term represents the Coulomb force $\vec{F_C}$. It linearly accelerates the particle (anti-) parallel to the field vector $\vec{E}$, depending on the particle's charge sign. The second term, called Lorentz force $\vec{F_L}$, is proportional to the particle charge and velocity. Due to the vector product, the resulting Lorentz force is orthogonal to the plane defined by $\vec{v}$ and $\vec{B}$. Thus, the particle path is deflected laterally, reaching the maximal value of deflection when velocity and magnetic field vectors are orthogonal and vanishes if they are parallel. A constant magnetic field does not alter the particle energy. To understand this, consider the following:

$$dW = \vec{F} \cdot d\vec{r} = \vec{F} \cdot \vec{v}\ dt = q\ (\vec{v} \times \vec{B}) \cdot \vec{v}\ dt = 0 \tag{2.19}$$

This equation tells us that the kinetic energy and, therefore, the velocity of the particle do not change when it traverses a constant magnetic field.
Now what happens, when a particle enters a constant, spatially homogeneous magnetic field? The motion has a circular path (Fig. 2.3).
This is due to the Lorentz force, which acts as a centripetal force. The particle traverses the circular path with a frequency $\omega = \frac{q}{m}B$, which is called Larmor frequency.
For a constant magnetic field, only particles with a certain momentum can occupy circular orbits of a certain radius R_0. The dependency may be calculated by equating the Lorentz force with the general expression for centripetal forces

$$F_\perp = F_L \tag{2.20}$$
$$m\tfrac{v^2}{R_0} = qvB \qquad , \ (\vec{v} \perp \vec{B}) \tag{2.21}$$
$$\Rightarrow mv = p = qBR_0 \tag{2.22}$$

or in natural units:

$$\frac{p}{keV} = 0.3\frac{B}{mT}\frac{R_0}{mm} \tag{2.23}$$

As stated before, the Lorentz force does not perform work, it does not change energy and speed of the particle. However, the particle is accelerated in the magnetic field, which leads to the emission of synchrotron radiation. Charged particles that are accelerated in a direction that is orthogonal to their velocity vector ($\vec{v} \perp \dot{\vec{v}}$) radiate the power

$$P \sim \frac{q^2}{c^3}\gamma^4(\dot{v})^2 \tag{2.24}$$

Which influence does the emission of synchrotron radiation have?

2.2.1. Particle's momentum measurement in CMS and tracking detectors

The charged particles crossing the CMS detectors leave ionization signals that are reconstructed as hits (cross symbols in figure 2.4). Using these spatial information, a track can be reconstructed by fitting the points with an helix-line. In the transversal view it assumes the shape of an arc of a circumference of length **L** and radius **R**. What is actually measured rather than the radius is the sagitta **s**, which is the maximal distance the track has from the straight line connecting the first and the last hits.

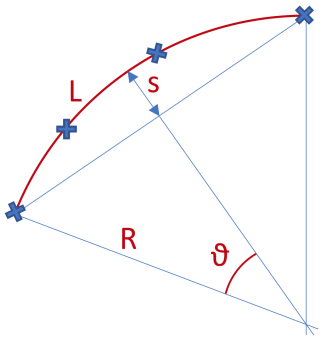

Figure 2.4.: Momentum measurement for charged particles in the CMS experiment.

Considering the θ angle small, the sagitta results:

$$s = R(1 - cos\theta) \approx \frac{R\,\theta^2}{2} = \frac{L^2}{8R} \tag{2.25}$$

So, obtaining R from the previous equation and substituting it into the generic momentum equation 2.23, we get the momentum equation depending on L, s and B:

$$p = 0.3\,B\,R \approx= 0.3\,B\,\frac{L^2}{8s} \tag{2.26}$$

2.3. Energy loss of electrons in matter

When particles traverse matter, they lose energy. This energy loss is caused by multiple effects. Particles may interact with shell electrons which causes excitations or even ionization. They may also interact with atomic nuclei, mostly by Coulomb scattering, which leads to the emission of Bremsstrahlung. If a charged particle travels at a speed higher than the speed of light in the corresponding medium ($c' = \frac{c}{n}$), Čerenkov radiation is emitted.
In this experiment, ionization and Bremsstrahlung are especially important. They are explained in more detail below.

2.3.1. Ionization

While the derivation of the formula of the energy loss for electrons and heavier particles in matter is different, the general approach is the same. Therefore, we will classically calculate the energy loss of heavy particles with $m \gg m_e$ by ionization and then the result will be translated for electrons. The derivation rests on the assumption that the energy of the incoming particle is much larger than the binding energy of the shell electron. Then, if the relative momentum transfer $\frac{\Delta p}{p}$ is small, the electron may be considered free and the trajectory of the heavy particle is a straight line.

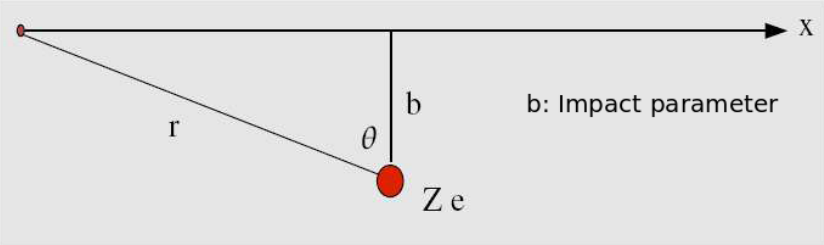

Figure 2.5.: Impact parameter definition.

When a particle with charge $Z_1 e$ passes close to the atom, the shell electron experiences a Coulomb force according to

$$\vec{F}_C = \frac{1}{4\pi\epsilon_0}\frac{Z_1 e}{(r^2)}\vec{e_r} \ . \tag{2.27}$$

The momentum transferred to the electron is

$$\Delta\vec{p} = \int_{-\infty}^{\infty} \vec{F}_C dt = \frac{e}{v}\int \vec{E}_\perp dx \tag{2.28}$$

where the longitudinal force component cancels because $\vec{F}_{C\parallel}(-x) = -\vec{F}_{C\parallel}(x)$. We use Gauss divergence theorem, obtaining

$$\Delta p = \frac{Z_1 e^2}{2\pi\epsilon_0}\frac{1}{bv} \ . \tag{2.29}$$

where b is the so called impact parameter, which quantifies the minimal distance between electron and incoming particle (see fig. 2.5).
The combined energy transfer to all electrons is calculated by integrating over all electrons in the volume dV. Using cylinder coordinates, we write

$$\Delta E = \frac{(\Delta p)^2}{2m_e} n_e dV = \frac{Z_1^2 e^4 n_e}{8m_e\pi^2\epsilon_0^2\beta^2c^2b^2}\, b\, d\phi db dx \tag{2.30}$$

where n_e is the electron density and $\beta = \frac{v}{c}$. The energy transfer per unit length is

$$\frac{dE}{dx} = \frac{e^4 Z_1^2 n_e}{4\pi\epsilon_0^2 m_e\beta^2c^2} \ln\frac{b_{max}}{b_{min}} \tag{2.31}$$

The maximal momentum therefore energy transfer is realized in central collisions, for which we obtain from eq. 2.29

$$\Delta p = 2m_e c\beta = \frac{Z_1 e^2}{2\pi\epsilon_0\beta c b_{max}} \tag{2.32}$$

$$\Rightarrow b_{max} = \frac{Z_1 e^2}{4\pi\epsilon_0 m_e c^2\beta^2} \tag{2.33}$$

The minimal energy transfer is the amount of energy necessary to ionize the electron. Therefore,

$$b_{min} = \frac{Z_1 e^2}{2\pi\epsilon_0\beta c}\frac{1}{\sqrt{2m_e I}} \tag{2.34}$$

where I is the mean ionization energy, which is about 163 eV for aluminum. For heavier elements, the average ionization energy may be approximated using

$$I = 9.73Z + 58.8Z^{-0.19}\text{eV}, \tag{2.35}$$

or for composites

$$\ln I = \sum_k g_k \ln I_k \tag{2.36}$$

where g_k is the ratio of electrons in atoms of kind k to the total number of electrons. Putting this into 2.31 yields

$$\frac{1}{\rho}\left(\frac{dE}{dx}\right)_{Ion} = \frac{Z_1^2 e^4}{8\pi\epsilon_0^2 m_e c^2}\frac{1}{\beta^2}\frac{Z}{A}N_A \ln\left(\frac{2m_e\beta^2c^2}{I}\right) \tag{2.37}$$

for the energy loss per unit length in $[\frac{dE}{dx}]$ = MeV cm^2/g. The electron density was replaced by $n_e \approx \frac{Z}{A}\rho N_A$, where A is the nucleus mass number and Z is the nuclear charge of the traversed material, which has a density ρ. The equation tells us that the energy loss depends on the speed ($\propto \frac{1}{\beta^2}$) and charge ($\propto Z_1^2$), but not the mass of the particle. The traversed material is considered in the factors $\frac{Z}{A}$ and $\ln(\frac{1}{I})$. Since scattering is a stochastic process, the formula only gives the average energy loss per unit length.
Now what changes when the incoming particle is an electron? Since the scattering partners are now equally heavy, the incoming particle does not follow a linear trajectory. Also, the scattering partners are quantum-mechanically identical particles, which makes a matching between initial and final state particles impossible. Here, we use the formula developed by Rohrlich and Carlson in 1954. It expands on work by Bethe.

$$\left(\frac{dE}{dx}\right)_{ion} = \frac{2\pi N_A r_0^2 m_e c^2}{\beta^2}\frac{Z\rho}{A}\left(\ln(\frac{\tau^2(\tau+2)}{2(I/m_e c^2)^2}) + \frac{\tau^2/8 - (2\tau+1)\ln 2}{(\tau+1)^2} + (1-\beta^2) - \delta\right) \tag{2.38}$$

Where $r_0 = \frac{e^2}{4\pi\epsilon_0 m_e c^2}$ is the classical electron radius and τ is the kinetic energy of the primary electron divided by $m_e c^2$, or simply $\tau = \gamma - 1$. δ is a density correction factor that represents the polarisation of the material caused by the electric charge of the traversing particle. For large distances, this causes a screening of the shell electrons. This effect is important for large energies and reduces the energy loss of the electron.

2.3.2. Bremsstrahlung

When charged particles are accelerated in the Coulomb field of atom nuclei, they emit Bremsstrahlung radiation. The emission is suppressed by the particle mass and thus only plays a role for light particles such as electrons. The average energy loss per unit length due to Bremsstrahlung is

$$\left(\frac{dE}{dx}\right)_{Brems} = 4\alpha N_A \frac{Z^2}{A} r_e^2 \ln\left(\frac{183}{Z^{\frac{1}{3}}}\right) E = \frac{E}{X_0}, \tag{2.39}$$

$$X_0 = \frac{A}{4\alpha N_A Z^2 r_e^2 \ln\left(\frac{183}{Z^{\frac{1}{3}}}\right)} \tag{2.40}$$

where $\alpha = \frac{1}{137}$ is the fine-structure constant. The energy loss is proportional to the initial energy of the incoming electron. X_0, called radiation length, is commonly given in $\frac{g}{cm^2}$.

It is the length after which the energy of the electron is attenuated by a factor $1/e \approx 37\%$.

The energy loss by ionization rises logarithmically at high energies, while Bremsstrahlung increases linearly. Thus, above some critical energy E_C the energy loss is dominated by Bremsstrahlung. For electrons in materials that are heavier than aluminum the critical energy may be determined using

$$E_C = \frac{800MeV}{Z + 1.2} \tag{2.41}$$

For composite substances, the average energy loss may be calculated as a combination of the individual losses for each of the components weighted with the corresponding mass fraction.

$$\frac{dE}{dx}_{tot} = \sum_i w_i \left(\frac{dE}{dx}\right)_i \tag{2.42}$$

2.4. Multiple scattering

When a particle traverses matter, many scattering processes occur. Each of the scattering events may change the travel direction of the particle (Fig. 2.6). Charged particles mainly scatter with the Coulomb field of the nuclei. This process causes the collimated incoming particle beam to expand in the medium. This affects the possible resolutions in detectors. Momentum measurements depend on the bending radius of charged particles in magnetic fields, which again depends on a precise spatial resolution. Since the actual travel distance in the material is unknown, dE/dx measurements are also distorted.

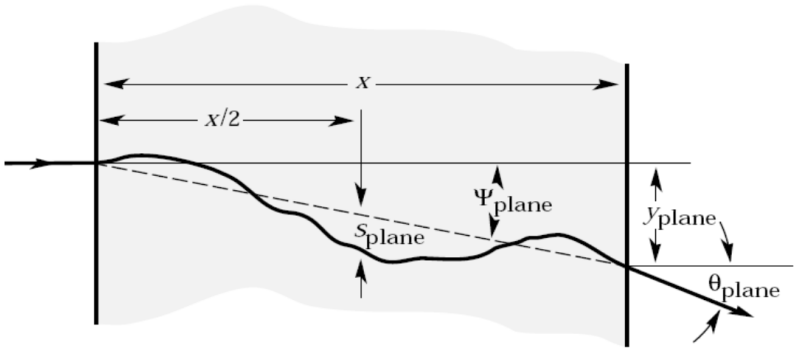

Figure 2.6.: Scattering in matter causes changes in travel direction of incoming particles.

This process is especially important for electrons. Their low mass facilitates large momentum transfers and thus large changes in travel directions. The effect of multiple scattering is described by Molière scattering theory. It states that the angular distribution is gaussian for small total scattering angles. This may be understood by thinking

of the total scattering angle as a superposition of many randomly distributed individual scattering angles. The Central Limit Theorem then states that the superposition is distributed according to a gaussian.
In this experiment, there are no mono-energetic electron sources, but a qualitative measurement of the effect may also be performed using a β-source.

3. Experimental setup

The experimental setup for performing the three measurements of this experiment is presented in figure 3.1.

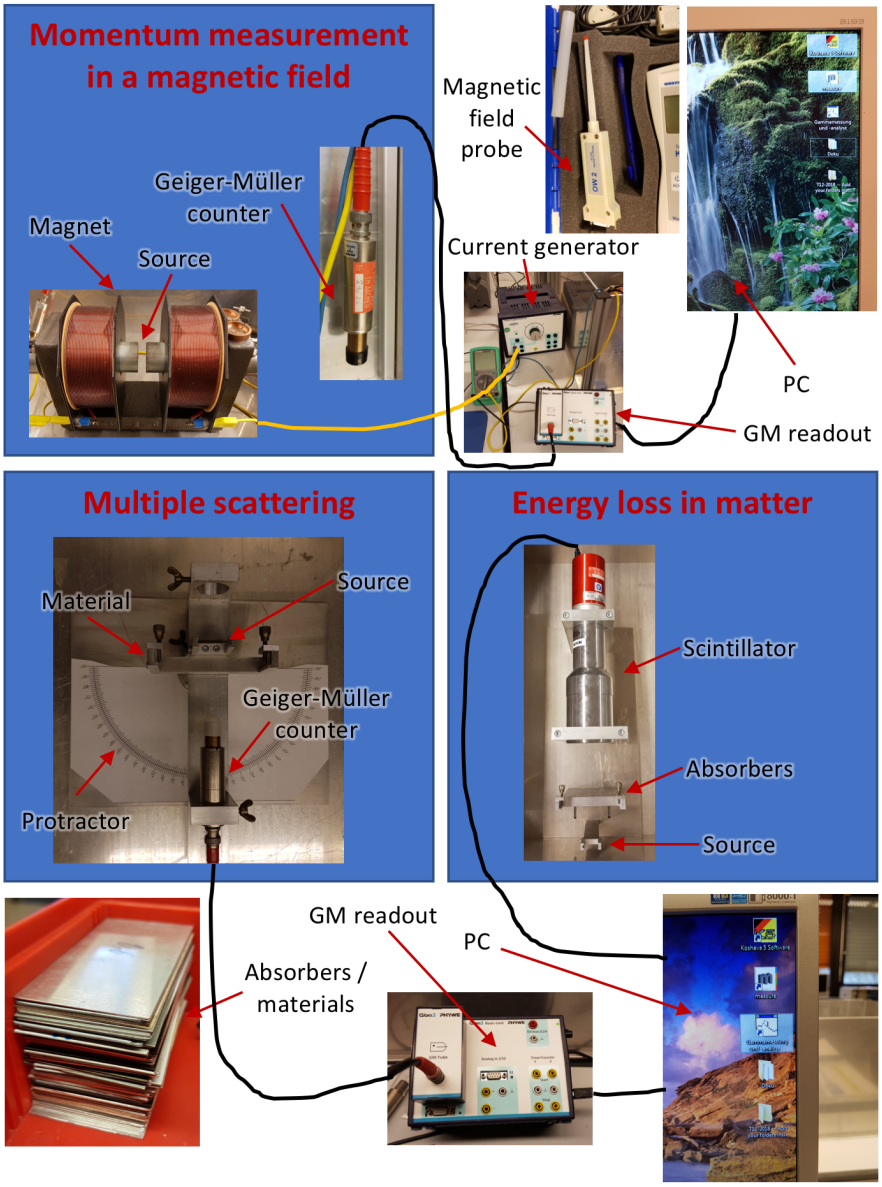

Figure 3.1.: Experimental setup. The three measurements will be performed using the apparatus contained in each of the drawn boxes.

3.1. Detection devices for nuclear radiation

In this experiment, you are going to use two ways of measuring electrons emitted by the ^{90}Sr source: a Geiger-Müller counter and a scintillator. In the following sections, both detectors are explained.

3.1.1. Geiger-Müller counter

Geiger-Müller (GM) counters are among the oldest types of detection devices for nuclear radiation. They consist of a metal cylinder serving as a cathode and a thin wire inside the cylinder serving as an anode. Modern GM counters have a window covered with a low-mass layer (e.g. Glimmer), which improves the detection efficiency. The cylinder is filled with a counting gas, which is a combination of a noble gas and a so called quenching gas. When ionizing particles traverse the volume, the gas is ionized along the particle path. The free electrons move towards the anode and cause a measurable current.
Depending on the applied voltage, the counter may be used in different ways.

The different working points are shown in fig. 3.2. In the recombination region, most

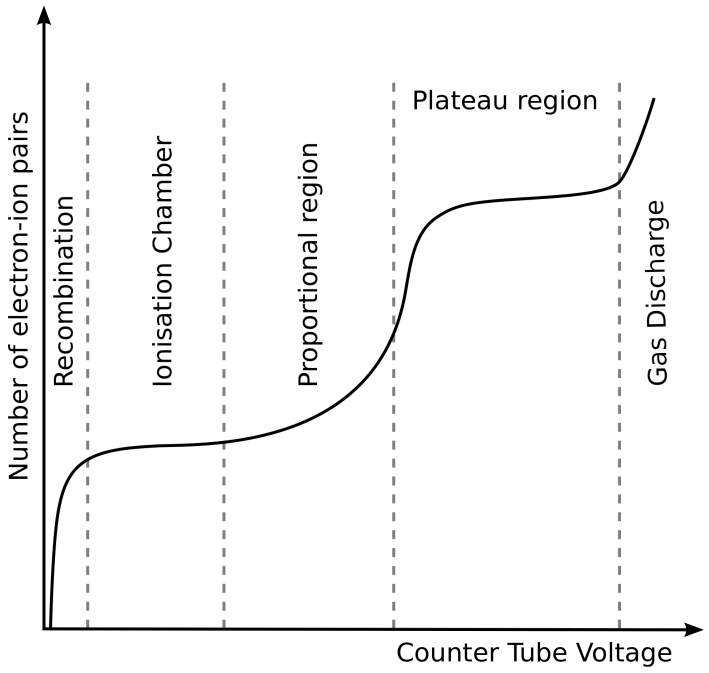

Figure 3.2.: Different operation regions of counter tubes.

electrons recombine with gas positive ions before reaching the anode. Above the recombination region, the counter may be used as an ionization chamber. Here, all electrons reach the anode and the measured current is proportional to the energy deposition of the ionizing particle.
At higher voltages, the proportional and gas amplification regions are reached. The strong electric field close to the anode accelerates the electrons in such a way that they

again ionize the gas. The measured current pulse is still proportional to the energy deposition, but it is amplified. Proportional counters can be used to distinguish α- and β-radiation.
At even higher voltages, the amplification becomes so strong that an ionization avalanche covers the whole volume. The discharged state persists until the cloud of gas ions has traveled far enough towards the cathode to screen the electric field. The quenching gas prevents an additional firing of the tube. The measured current is now independent of the energy deposition and all particles cause the same signal.
In this experiment, we use a GM counter, that is read out using a Cobra3 system. Voltage supply and signal output use a BNC cable. A voltage of 500 V is supplied.

3.1.2. Scintillators

Scintillators are among the most used detectors for nuclear radiation.

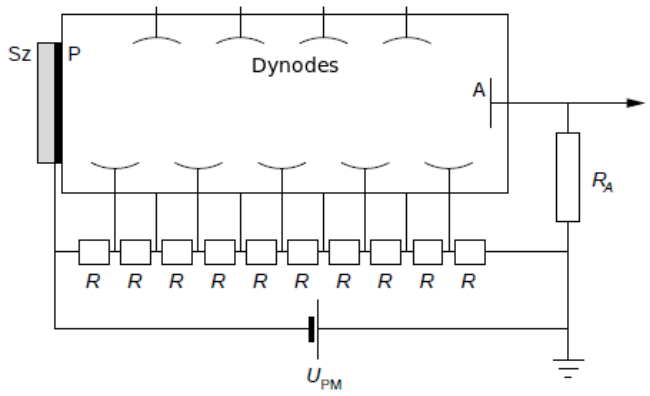

Figure 3.3.: Schematic drawing of scintillator and photomultiplier.

A schematic drawing is shown in fig. 3.3. In the scintillating material (Sz), ionizing radiation causes light flashes, which release electrons from the photo cathode P. Using a system of dynodes, which initiate emission avalanches, the number of photo-electrons is multiplied, thus amplifying the signal. The resulting voltage pulse is proportional to the energy deposition. The scintillation material should absorb as much of the energy of traversing particles as possible. The conversion fraction of traversing energy to light energy is called light yield. A linear relationship between the deposited energy amount and the number of scintillation photons is desirable to ensure a linear current response in the following. The scintillator should also be transparent to the scintillation light.

There are two types of scintillators with individual advantages. There are organic scintillator (e.g. plastic), which are very fast and only have small dead times. However, they have a bad energy resolution. Organic scintillators are commonly used as triggers for other detectors.
The second kind are inorganic scintillators such as NaI(Tl) or CsI, which have good energy resolution, but they are slow. In this experiment, a thallium doped sodium iodide scintillator is used. It has a very good light yield in the whole relevant spectral region (see fig. 3.4.
On the other hand, NaI(Tl) is fragile and hygroscopic, which makes insulation from air necessary. Due to their regular structure, inorganic crystals have pronounced band structure features. The scintillation process can thus be described using the band model (see fig. 3.5).
The valence band contains electrons bound to individual molecules, while the conduction band is filled with electrons which are free within the material. When energy is deposited in the crystal, electrons are lifted from the valence into the conduction band. When the electrons fall back to the valence band, a photon with energy E_1 is emitted. Since this energy corresponds to the difference between valence and conduction band

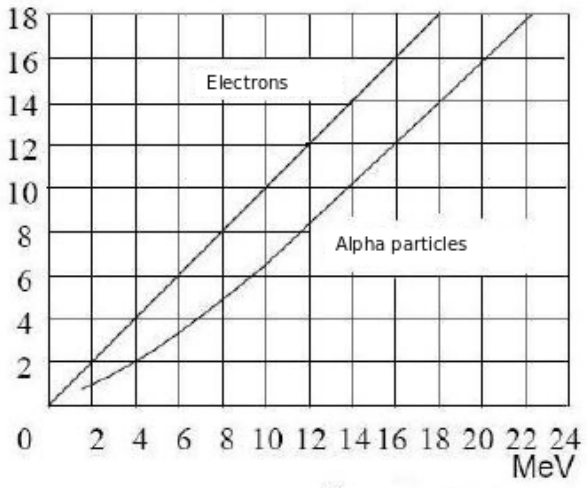

Figure 3.4.: Light yield of electrons and α-particles depending on their kinetic energy.

levels, the photon can be absorbed again. Thus, the material is opaque to the photon. To prevent this, activator atoms (here: thallium) are introduced into the crystal. The activator atoms cause additional energy levels close to the conduction band to be created. Electrons in the conduction band can now return to the valence band in two steps. They first fall into the activator states, which causes a phonon, but no photon to be created. In a second step they fall down from the activator states to the valence band, which causes emission of a photon. The photon now has an energy E_2 which is too small to cause additional excitations. The material is thus transparent to the photon.

3.2. Momentum resolution

The setup for this experiment is shown schematically in figure 3.6. Electrons are produced in the source S and pass through an opening of width Δx_1 into the magnetic field. Here, they are deflected and detected using the detector D. In front of the detector, there is a cover with an opening of width Δx_2. Determine the momentum resolution assuming that electrons enter the magnetic field parallel to the x direction.

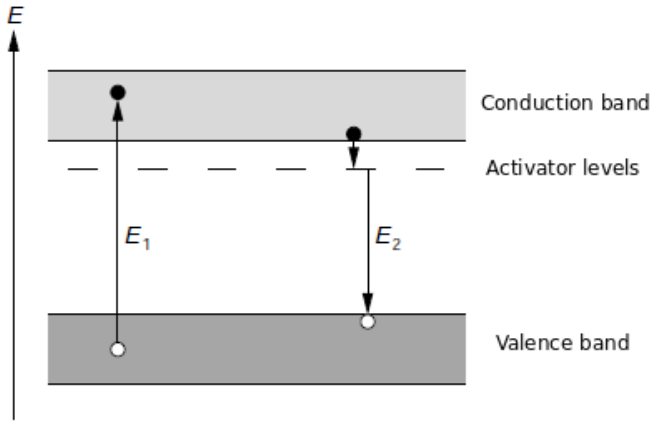

Figure 3.5.: Scintillation process of an inorganic scintillator visualized using the band model.

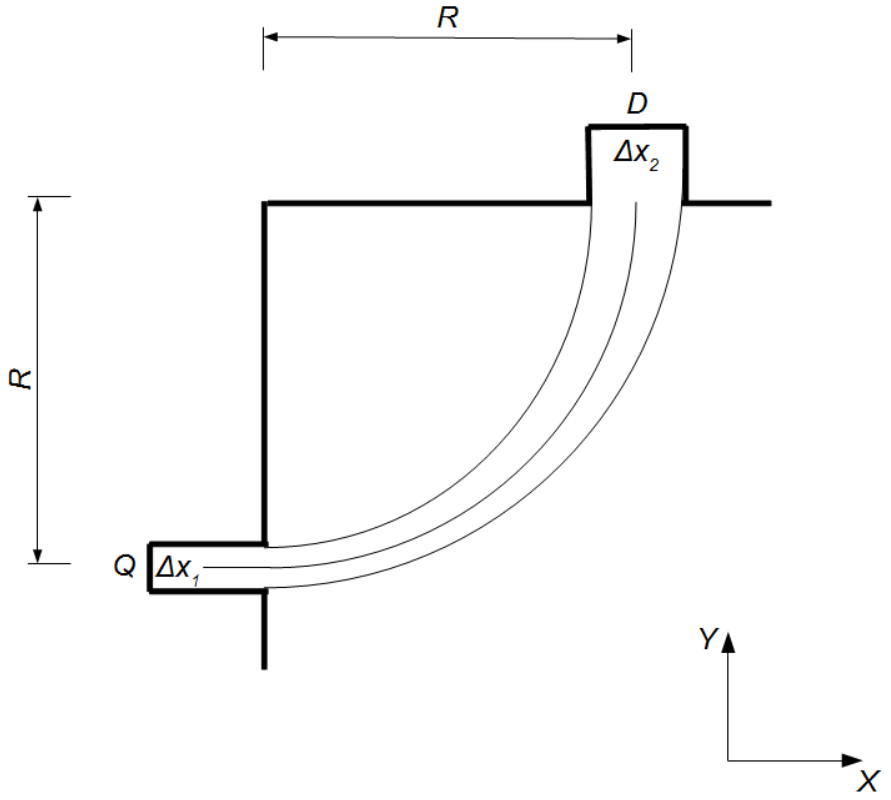

Figure 3.6.: Schematics of a momentum spectroscope.

4. Execution

4.1. Momentum measurement in a magnetic field

0. Always modify **slowly** the current feeding the coils of the magnet to reduce the probability to have residual magnetic field at zero current ($B_M = 0$ at $I_M = 0$). **The current must always be set to a value lower than $5\mathbf{A}$ ($I_M < 5\mathbf{A}$).** In addition, check that the aperture between the two poles of the magnet is less than 0.5 - 1 cm... Why?

1. Use the hall probe to measure the magnetic field between the pole pieces of the electromagnet; the grid drawn on the surfaces serve as a reference. Check where the magnetic field is homogeneous and how different currents affect the temporal behavior of the field. To do this, perform 60 seconds long measurements for different currents (sampling every 0.2 sec or whatever you find reasonable). **Attention**: connect the hall probe to the USB port on the right.

2. Use the available supplies to construct a setup for the measurement of the momentum spectrum of ^{90}Sr. Take care to choose a sensible and convenient position for source and GM counter. **Ask your supervisor to check the setup before putting it into operation!**

3. Measure the count rates in dependence of the magnetic field. Vary the field in appropriate steps. The settings of the power supply might be too coarse to vary the field as precisely as you would like. In this case, use the pole piece screw to adjust the field. Always keep the Hall probe into the aperture between the poles, in a fixed position OUTSIDE the electron path! If the value you get is slightly different from the one in the center of the magnet, you have to rescale it: use the field map measured in the point 1.

4. To estimate background levels, measure the count rate without a magnetic field. **Correct your measurement accordingly.**

Note: The available hall probe works in transversal mode. Its measurement range is either $0 - 2$mT or $0 - 2$T. Depending on the chosen settings, it can measure constant or time dependent fields. Software to extract measured data is available.

4.2. Energy loss in matter

0. **Do not change the supply voltage (500V)**. Turn on the HV after having opened the program and turn it off before closing it.

1. When you collect the data, always check to have enough statistics. **Tip**: Save the data in .TKA extension, which corresponds to an easy readable text file...

2. Measure the spectrum of ^{90}Sr without any absorber. **Adjust the amplification factor such that the complete spectrum is recorded**.

3. Measure the spectra of ^{22}Na, ^{137}Cs, ^{60}Co and ^{152}Eu. These should enable you to do an energy-to-channel calibration.

4. Measure also the background... And use it properly!

5. Measure the spectra of the ^{90}Sr with the aluminium absorbers of different thicknesses (at least 4 $\rightarrow$ 0mm not included!).

4.3. Multiple scattering

1. Install the GM counter in its mount. It may be necessary to restart the Measure software. Take off the plastic cover and put on the collimator (metal piece) with the opening in a perfect vertical position.

2. Measure the angular distribution of the electrons for the ^{90}Sr and the ^{204}Tl sources without and with absorbers, choosing reasonable angular steps based on how you expect the distribution is. At least you should use 4 different thicknesses of aluminum and 4 different materials with the same thickness (compare it to the aluminum if it is not clear what is the size). Take care to choose sensible measurement times and consider the measurement of the background.

3. **Attention**: The Thallium source could have a low activity; if it is impossible to measure anything, call the tutor and decide what is better to do.

5. Analysis

- Present the measured magnetic field properties appropriately and discuss them. Is the magnetic field sufficiently homogeneous or do you need to use an effective average? Where does the magnetic field become inhomogeneous?
- Plot the momentum and energy spectra. Transform the spectrum into a Kurie diagram, with and without Fermi correction. Use it to determine the maximal energy of the spectrum and estimate the uncertainty of $E_{\max}$. What effect does the Fermi correction have?
- Perform an energy-to-channel calibration for the scintillator.
- Plot the measured energy spectra. Present all spectra with aluminum absorbers in the same diagram. Do the same for the spectra with absorbers of the same strength. Once again, create Kurie diagrams and determine $E_{\max}$ and its uncertainty.

  The aluminum shielding has a nominal area mass density of $X = 147\frac{\text{mg}}{\text{cm}^2}$. The scintillator crystal is covered by an aluminum-oxide reflector with density $\rho = 3.94\text{g/cm}^3$. The reflector is meant to prevent scintillation photons from leaving the scintillation volume, thus increasing the light yield. It has a nominal thickness of 1.6 mm and an area mass density of $88\frac{\text{mg}}{\text{cm}^2}$. The reflector and aluminum shielding must be considered in the analysis of your data.

  - Compare your results to theory.
  - Are the nominal specifications correct?
  - Discuss your results.
- Plot the measured angular distributions in the same diagram. Is the angular distribution compatible with a gaussian distribution (χ^2/N_{dof})? Look at the difference between the distributions with and without absorbers. Is the difference distributed according to a gaussian, too?
- You have measured the maximal energy and momentum of charged particles. Calculate the particle mass! Discuss uncertainties. Can this result be used to identify the particles?
- Briefly discuss how these measurement methods are used in modern detectors. What does this tell us about a "good" detector?
- To what class does the transition from ^{90}Y to ^{90}Sr belong?

Many of the results from this experiment will have limited precision (e.g. the mass measurement). Your analysis should focus on correct handling of uncertainties. It should reflect your understanding of principles and methods. Many plots can be put into the same figure. Important results should be given in the text or in tables.

Appendices

A. Useful plots

A.1. Sources

The gamma emitters Na22, Cs137, Co60 and Eu152 are used for energy calibration. The used β-sources are Sr90 and Tl204 with activities of 360 kBq and 12 kBq, respectively. Their decay schemes are shown in fig. A.1.

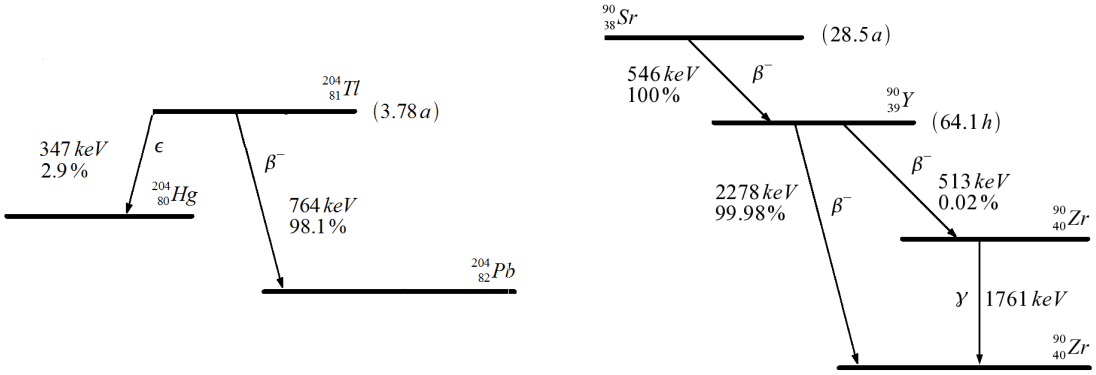

Figure A.1.: Decay scheme of Tl204 und Sr90.

A.2. Fermi integral

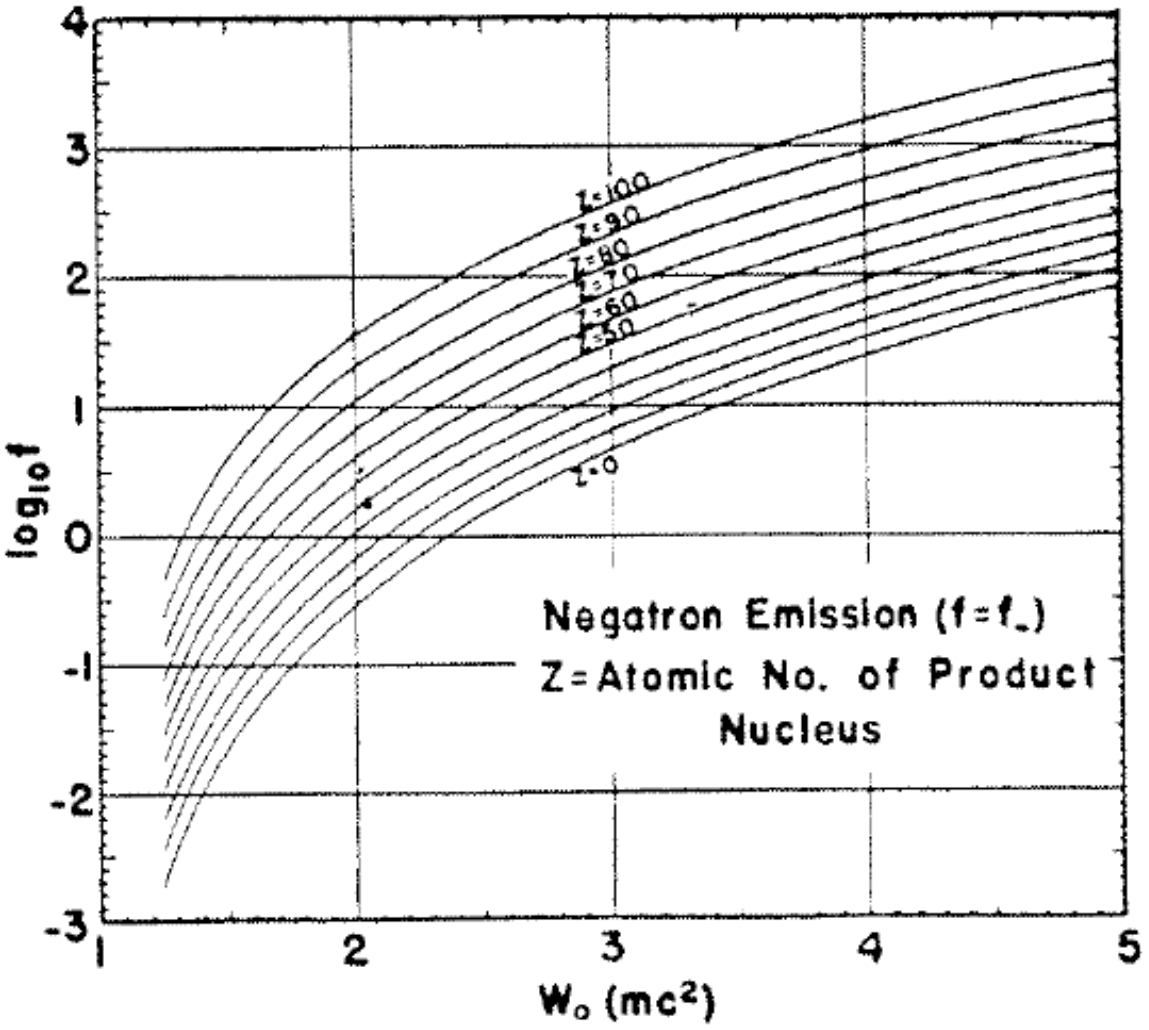

Figure A.2.: Logarithmic view of β^-decay spectra at different nuclear charges.

B. Charged particles in magnetic fields: equation of motion

In this appendix, we want to go though the computation of the equation of motion of a particle inside a constant magnetic field (Fig. 2.3).

Without loss of generality, we choose our coordinate system such that

$$\vec{v} = \begin{pmatrix} v_0 \\ 0 \\ 0 \end{pmatrix}, \ \vec{B} = \begin{pmatrix} 0 \\ 0 \\ B \end{pmatrix} \tag{B.1}$$

which gives us the equation of motion

$$m \ \ddot{\vec{x}} = q \ \vec{v} \times \vec{B} \tag{B.2}$$

with the initial conditions

$$x(0) = 0, \ y(0) = 0, \ \dot{x}(0) = v_0, \ \dot{y}(0) = 0 \tag{B.3}$$

where $t = 0$ is the time at which the electron enters the magnetic field. We suppress explicit time dependencies and write the separate components:

$$\ddot{x} = \frac{q}{m} B\dot{y} \tag{B.4}$$

$$\ddot{y} = -\frac{q}{m} B\dot{x} \tag{B.5}$$

This is a system of coupled differential equations. Performing time integration yields

$$\dot{x} = \frac{q}{m} By + C_1 \tag{B.6}$$

$$\dot{y} = -\frac{q}{m} Bx + C_2 \tag{B.7}$$

where the integration constants $C_1 = v_0$ and $C_2 = 0$ are determined from the initial conditions $\dot{x}(0) = v_0, \ y(0) = 0$ and $\dot{y}(0) = 0, \ x(0) = 0$. By putting eq. B.7 into B.4, the differential equations are de-coupled:

$$\ddot{x} = -(\frac{q}{m} B)^2 x \tag{B.8}$$

Equation B.8 describes a harmonic oscillation and is solved by

$$x(t) = A_1 \cos wt + A_2 \sin wt, w = \frac{q}{m}B \tag{B.9}$$

Using the initial condition $x(0) = 0$, we get $A_1 = 0$. Also, we deduce $\dot{x}(0) = v_0 \Rightarrow A_2 = \frac{v_0}{w}$ and arrive at

$$x(t) = \frac{v_0}{w} \sin wt \tag{B.10}$$

We put B.10 into B.7 and get

$$\dot{y} = -v_0 \sin wt \tag{B.11}$$

integrating one more time yields

$$y(t) = \frac{v_0}{w} \cos wt + C_3 \tag{B.12}$$

Where we have determined $C_3 = -\frac{v_0}{w}$ from $y(0) = 0$.

$$y(t) = \frac{v_0}{w}(1 - \cos wt) \tag{B.13}$$

The final solution is then

$$\vec{r} = \begin{pmatrix} x(t) \\ y(t) \\ z(t) \end{pmatrix} = \begin{pmatrix} \frac{v_0}{w} \sin wt \\ \frac{v_0}{w}(1 - \cos wt) \\ 0 \end{pmatrix} \tag{B.14}$$

As we expected, this equation of motion describes a circular path. This is due to the Lorentz force, which acts as a centripetal force.